

# CMOS-Compatible Deposited Materials for Photonic Layers Integrated above Electronic Integrated Circuit

Shiyang Zhu, G. Q. Lo, and D. L. Kwong

**Abstract**—Silicon photonics has generated an increasing interest in recent years mainly for optical communications optical interconnects in microelectronic circuits or bio-sensing applications. The development of elementary passive and active components (including detectors and modulators), which are mainly fabricated on the silicon on insulator platform for CMOS-compatible fabrication, has reached such a performance level that the integration challenge of silicon photonics with microelectronic circuits should be addressed. Since crystalline silicon can only be grown from another silicon crystal, making it impossible to deposit in this state, the optical devices are typically limited to a single layer. An alternative approach is to integrate a photonic layer above the CMOS chip using back-end CMOS fabrication process. In this paper, various materials, including silicon nitride, amorphous silicon, and polycrystalline silicon, for this purpose are addressed.

**Keywords**—Silicon photonics, CMOS, Integration.

## I. INTRODUCTION

SILICON photonics has generated an increasing interest in recent years mainly for optical communications optical interconnects in microelectronic circuits or bio-sensing applications. The development of elementary passive and active components (including detectors and modulators), which are mainly fabricated on the silicon on insulator platform for CMOS-compatible fabrication, has reached such a performance level that the integration challenge of silicon photonics with microelectronic circuits should be addressed [1]. Since crystalline silicon can only be grown from another silicon crystal, making it impossible to deposit in this state, the optical devices are typically limited to a single layer. Therefore, the photonic devices are integrated on an electronic wafer either by fabrication of transistors and photonic devices in the same layer (monolithic integration) or by wafer bonding of the separately fabricated photonic circuit and electronic circuit (heterogeneous integration). These two approaches have their own advantages and disadvantages. Moreover, the SOI process typically raises the cost of a wafer by at least an order of magnitude, and limits the architecture to a single

optical layer.

An alternative approach to integrate a photonic layer into CMOS technology is to include it in the same manner as an additional metallic layer in the Si CMOS process flow, i.e., on the top of the stacked layers that have been used for the electrical interconnect, as shown schematically in Fig. 1. A major benefit of this approach is that multiple photonic layers can be stacked with a buffer layer of cladding material in between them. A critical constraint of this approach is the thermal budget, which should be compatible to the CMOS back-end process, i.e., less than 400°C.

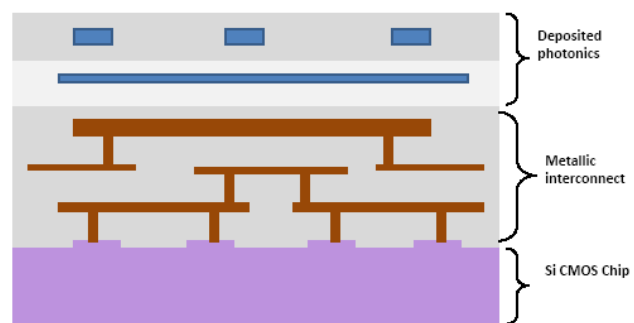


Fig. 1 Cross-sectional view of deposited photonic layers, which are fabricated above the Cu/low-k based metallic interconnect layer of Si CMOS chip

The cladding layer is naturally  $\text{SiO}_2$  which has the refractive index of 1.44. The materials for waveguide core should have refractive index larger than 1.5 and be transparent at 1.55- $\mu\text{m}$  wavelengths. The candidates reported to date include  $\text{SiN}$ , amorphous-Si (a-Si), polycrystalline-Si (poly-Si),  $\text{AlN}$ , and  $\text{TiO}_2$ , etc. The materials have their own advantages and disadvantages to be used as waveguides [2]. In this paper, the properties of  $\text{Si}_3\text{N}_4$ , a-Si, and poly-Si waveguides as well as other photonic devices based on these waveguides are presented.

## II. SILICON NITRIDE

$\text{Si}_3\text{N}_4$  has index of  $\sim 2.0$ . It can be deposited on almost any substrates using mature deposition technologies such as low press chemical vapor deposition (LPCVD) and plasma-enhanced chemical vapor deposition (PECVD). LPCVD  $\text{Si}_3\text{N}_4$  has been shown to have very low propagation loss of  $\sim 0.1$  dB/cm at 1.55  $\mu\text{m}$  wavelengths and PECVD  $\text{Si}_3\text{N}_4$  waveguides

Shiyang Zhu, G. Q. Lo, and D. L. Kwong are with the Institute of Microelectronics, A\*STAR (Agency for Science, Technology and Research), Singapore 117685, Singapore (corresponding author to provide phone: 65-67705746; fax: 65-67731914; e-mail: zhusy@ime.a-star.edu.sg).

This work was supported by the Science and Engineering Research Council of A\*STAR (Agency for Science, Technology and Research), Singapore Grant 092-154-0098.

have a slightly large propagation loss of  $\sim 1\text{--}2$  dB/cm due to absorption of Si-N and N-H bonds. Owing to the low propagation loss, various high-performance passive optical components such as filters have been demonstrated based on the  $\text{Si}_3\text{N}_4$  waveguides. However, due to the relatively small refractive index contrast between the  $\text{Si}_3\text{N}_4$  core and the  $\text{SiO}_2$  cladding, the  $\text{Si}_3\text{N}_4$  waveguide requires a relatively large size to confine the optical mode, which results in low integration density.

$\text{Si}_3\text{N}_4$  rib waveguides fabricated in this work have cross section as shown in Fig. 2 (a). The electric field distribution for 1550-nm fundamental TE mode is depicted in Fig. 2 (b). The calculated effective modal index is 1.626 and the ratio of optical power contained in the  $\text{Si}_3\text{N}_4$  core is 60% (i.e., the remaining 40% optical power is contained in the cladding  $\text{SiO}_2$  layer). The waveguides with different lengths are fabricated and are measured using different laser sources. The results are shown in Fig. 2 (c). The propagation loss is smaller than  $\sim 1$  dB/cm over a wide wavelength range, comparable to those reported in literature for single-mode  $\text{Si}_3\text{N}_4$  channel waveguides [3]. The loss increase in the C-band and the large loss ( $\sim 10.5$  dB/cm) at 420nm may be attributed to Si-H and N-H bonds in the film.

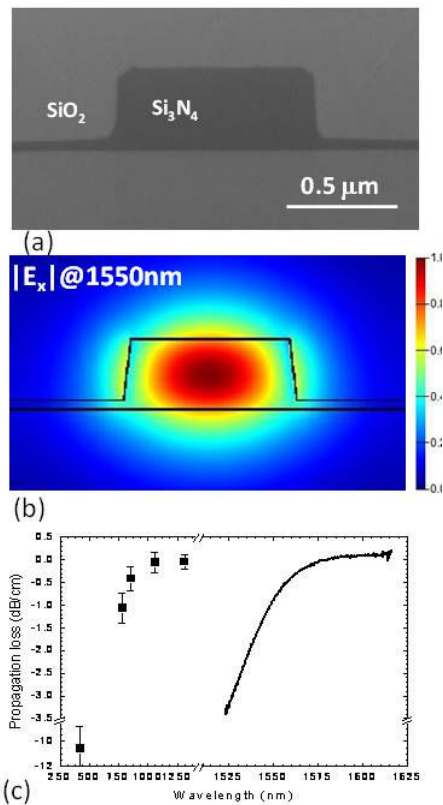


Fig. 2 (a) XTEM image of the  $\text{Si}_3\text{N}_4$  waveguide, (b) Electric field distribution for fundamental 1550 TE mode, and (c) Propagation loss at different wavelength, measured using the cutback method

Waveguide ring resonators are also fabricated, as shown in Fig. 3 (a). The ring resonator has radius of  $20\mu\text{m}$  and gap between the ring and bus waveguides of  $0.2\mu\text{m}$ . Fig. 3 (b) shows the measured through and drop spectra of the waveguide-ring resonator shown in Fig. 3 (a). We can see it exhibits typical resonant characteristics with Q-value of  $\sim 1100$  and free spectral range (FSR) of  $\sim 9.8\text{nm}$ , corresponding  $n_g$  of  $\sim 1.9$ .

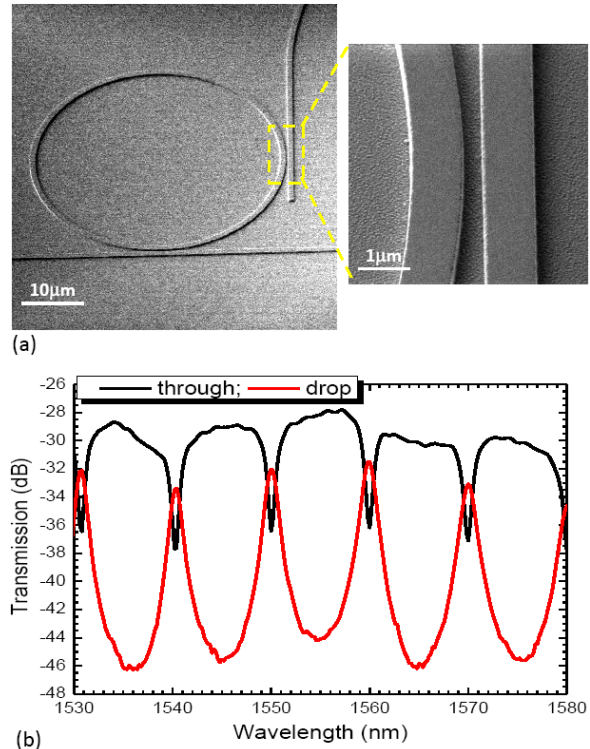


Fig. 3 (a) SEM image of a ring resonator based on  $\text{Si}_3\text{N}_4$  rib waveguide, the gap between the bus and ring waveguides is  $\sim 0.2\mu\text{m}$ ; and (b) The measured through and drop spectra

### III. AMORPHOUS SILICON

Hydrogenated amorphous silicon provides distinct advantages such as high refractive index ( $\sim 3.5$ , similar or even slightly larger than that of crystalline-Si), low absorption loss at  $1.550\mu\text{m}$  wavelengths, capability of PECVD deposition on almost any substrates, large nonlinear effect, and even possibility for active modulation and detection [4]. A very low propagation loss of  $\sim 2\text{--}3$  dB/cm at  $1550\text{nm}$  has been reported for a-Si:H wire waveguides [5], which is comparable to the crystalline Si counterparts with the same dimensions. The low optical loss of a-Si:H waveguides is mainly resulted from sufficient passivation of dangling bonds in a-Si. Therefore, the property of a-Si waveguides depends on the fabrication details. Fig. 4 (a) is the XTEM image of the fabricated a-Si waveguides. The measured output power is plotted in Fig. 4 (b) as a function of waveguide length for various a-Si waveguides. We can see that a very low loss of  $\sim 2.7$  dB/cm

has been measured for optimized deposition conditions (the S4 sample shown in the figure), but other a-Si waveguides exhibits relatively large propagation losses. Moreover, the a-Si waveguide will degrade during the subsequent heat treatment due to hydrogen diffuses out, as shown in Fig. 5 [6].

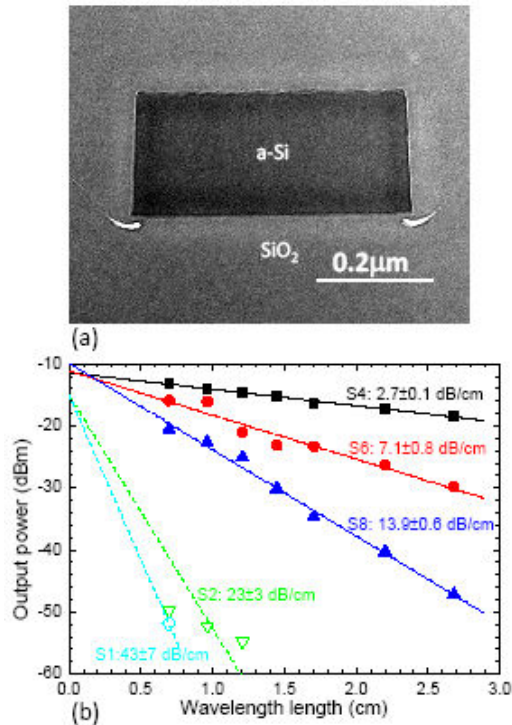


Fig. 4 (a) XTEM image of the fabricated a-Si:H waveguide; (b) Output light power versus waveguide length measured at 1550-nm TE light for a-Si:H waveguides with different fabrication parameters. The lowest propagation loss is  $\sim 2.7$  dB/cm

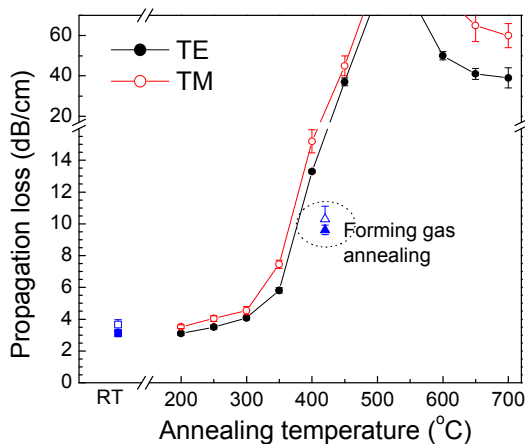


Fig. 5 The propagation loss of 220nm $\times$ 500nm a-Si:H wire waveguides as a function of subsequent furnace annealing temperature. The annealing temperature keeps 30 min. The initial propagation losses as well as those after the forming gas annealing are also shown for comparison

#### IV. POLYCRYSTALLINE SILICON

Poly-Si provides unique properties as it can be easily deposited on almost any substrates and simultaneously it has moderate carrier mobility capable for active photonic devices. Some examples include metal-oxide-semiconductor based electro-optic modulators, horizontal slot waveguides for electrical injection, three-dimensional photonic crystals with an infrared band gap, and poly-Si ring resonators. Poly-Si can be deposited directly in the polycrystalline phase at a temperature of  $\sim 620$ – $650^\circ\text{C}$  by LPCVD, or be deposited by LPCVD in the amorphous phase at  $\sim 530$ – $580^\circ\text{C}$  and subsequently solid phase crystallized (SPC) at higher temperatures. The SPC approach can provide superior poly-Si properties (e.g. smoother surface, higher structural perfection, etc.), in turn lower optical loss, than the directly deposited ones. It has been reported that the propagation loss is  $\sim 7$ – $9$  dB/cm for poly-Si waveguides formed by high-temperature ( $\geq 1000^\circ\text{C}$ ) / long-time (several hours) furnace annealing [7]. To reduce the required thermal budget, the effect of low temperature annealing (LTA), rapid thermal annealing (RTA), or a combination of both on the propagation loss have been studied. A relatively low propagation loss of  $\sim 9.8$  dB/cm is achieved by SPC of first LTA and then RTA [8]. Fig. 6 shows the experimental results of poly-Si wire waveguides after various SPC conditions. The propagation loss is  $\sim 9.8$  dB/cm after high-temperature annealing and is  $\sim 11.3$  dB/cm after low temperature annealing plus rapid thermal annealing.

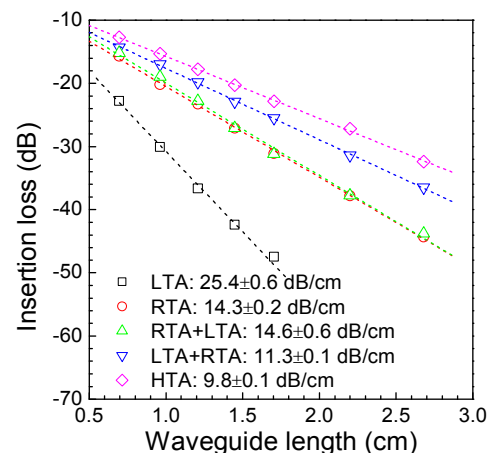


Fig. 6 Insertion losses of the  $0.22\mu\text{m}$  (height) $\times$  $0.3\mu\text{m}$  (width) polycrystalline Si wire waveguides with various SPC procedures as a function of their lengths

#### V. CONCLUSION

Three deposited materials for integrated photonics are addressed and compared, including  $\text{Si}_3\text{N}_4$ , a-Si, and poly-Si. The  $\text{Si}_3\text{N}_4$  waveguide provides the lowest propagation loss. However, it is difficult or even impossible to realize active function such as electro-optic modulation and detection based on this waveguide. On the other hand, both a-Si and poly-Si

are semiconductor, thus enabling to realize active functions. The amorphous-Si provides lower propagation loss than poly-Si, however, it is not thermal stable and it has much lower carrier mobility than poly-Si. Therefore, in the view of the active functions, the poly-Si may be the best of choice, while for the passive functions  $\text{Si}_3\text{N}_4$  is the best of choice. It indicates we need to integrate both  $\text{Si}_3\text{N}_4$  waveguide and poly-Si waveguide is the same integrated photonic chip.

## REFERENCES

- [1] D. J. Lockwood and L. Pavesi, "Silicon photonics II: components and integration", Topic in Applied Physics, vol. 119, Springer-Verlag, Berlin (2011).
- [2] A. Biberman, K. Preston, G. Hendry, N. Sherwood-Droz, J. Chan, J. S. Levy, M. Lipson, and K. Bergman, "Photonic network-on-chip architectures using multiple deposited silicon materials for high performance chip multiprocessors," ACM J. Emerging Technologies in Computing Systems, vol. 7, no. 2, art. 7 (2011).
- [3] A. Gondarenko, J. S. Levy, and M. Lipson, "High confinement micro-scale silicon nitride high Q ring resonator," Optics Express, vol. 17, pp. 11366-11370 (2010).
- [4] F. G. D. Corte, S. Rao, G. Coppola, and C. Summonte, "Electro-optical modulation at 1550 nm in an as-deposited hydrogenated amorphous silicon p-i-n waveguiding device," Optics Express **19**(4), 2941-2951 (2011).
- [5] S. Y. Zhu, G. Q. Lo, and D. L. Kwong, "Low-loss amorphous silicon wire waveguide for integrated photonics: effect of fabrication process and the thermal stability," Optics Express **18**(24), 25283-25291 (2010).
- [6] S. Y. Zhu, G. Q. Lo, W. Li, and D. L. Kwong, "Effect of cladding layer and subsequent heat treatment on hydrogenated amorphous silicon waveguides," Optics Express **20**(21), 23676-23683 (2010).
- [7] S. Y. Zhu, Q. Fang, M. B. Yu, G. Q. Lo, and D. L. Kwong, "Propagation losses in undoped and n-doped polycrystalline silicon wire waveguides," Optics Express **17**(23), 20891-20899 (2009).
- [8] S. Y. Zhu, G. Q. Lo, and D. L. Kwong, "Influence of RTA and LTA on the optical propagation loss in polycrystalline silicon wire waveguides," IEEE Photonics Technology Lett., **22**(2), 480-482 (2010).